First neutron spin-echo measurement at HANARO

Article *in* Journal- Korean Physical Society · April 2005

CITATIONS
0

READS
206

5 authors, including:

Changwoo Do
Oak Ridge National Laboratory
81 PUBLICATIONS **644** CITATIONS
SEE PROFILE

Dong-Cheol Woo
Asan Medical Center
100 PUBLICATIONS **411** CITATIONS
SEE PROFILE

Seong-Min Choi
Chonnam National University
167 PUBLICATIONS **1,105** CITATIONS
SEE PROFILE

Myungkook Moon
Korea Atomic Energy Research Institute (KAERI)
64 PUBLICATIONS **315** CITATIONS
SEE PROFILE

Journal of the Korean Physical Society, Vol. 46, No. 5, May 2005, pp. 1075∼1079

First Neutron Spin-Echo Measurement at HANARO

C. K. Doe, D. C. Woo and S. M. Choi*
Department of Nuclear and Quantum Engineering, Korea Advanced Institute of Science and Technology, Daejeon 305-701

M. K. Moon and C. H. Lee
Korea Atomic Energy Research Institute, Daejeon 305-600

(Received 12 November 2004, in final form 9 March 2005)

A neutron spin-echo instrument has been developed and tested at the ST-1 beam port of the High-flux Advanced Neutron Application Reactor (HANARO). The phase evolution of a neutron spin was directly observed with this neutron spin-echo instrument. Polarized thermal neutrons (λ = 1.2 Å, polarization $\cong$ 0.37) were produced by the (200) reflection plane of a $Co_{0.92}Fe_{0.08}$ ferromagnetic single crystal and were then transported to the experiment area of the ST-1 beam port. The efficiency of the developed spin flipper was estimated to be 0.98 ± 0.01, and the spin flipping ratio of the instrument was measured to be 1.26. The measured spin echo point was in agreement with the expected value. The spin-echo time of our instrument was estimated to be in the range of a few picoseconds.

PACS numbers: 03.75.Dg, 39.20.+q
Keywords: Spin-echo, Polarization, Neutron

I. INTRODUCTION

Due to the neutron's unique physical properties, neutron scattering is a powerful tool for investigating structures [1] and dynamics of materials. Especially, magnetic scattering using the spin angular momentum $\frac{\hbar}{2}$ of neutrons has been a great tool for understanding magnetism and superconductivity [2]. As spin phase control devices and instruments have been developed, a new type of neutron scattering method, called spin echo spectroscopy, has been introduced and has achieved neV energy resolution in neutron spectroscopy.

Hahn (1950) discovered that nuclear spins that have precessed differently in an inhomogeneous static field can be in phase after a certain RF pulse; he called such a phenomenon as a spin echo [3, 4]. Neutron spin-echo spectroscopy, which is an analogy to this phenomenon, was first introduced by Mezei [5,6]. In typical neutron spin-echo measurements, neutrons initially polarized in the z direction and traversing along the y direction are used. Along the beam path, there are various spin phase control devices. A spin flip coil, called a $\pi/2$ spin flipper, rotates the spins into the x-y plane by using a transverse field and initiates Larmor precession of the spins in the subsequent static magnetic field along the z direction. Going through a static field of fixed path length, the spin phases of neutrons with different velocities evolve different amounts and become out of phase. Next, a flipper coil called a π-spin flipper reverses the phase evolutions of neutron spins. After the π-spin flipper, neutron spins go through another static field of fixed path length where spin phases with different velocities again evolve different amounts. Since the phase evolution has been reversed by the π spin flipper before entering the second static field, the latter phase evolution, combined with the prior phase evolution, results in an in-phase situation of neutron spin phases. Therefore, a full polarization can be observed at the end. This recovered polarization is often called a spin-echo signal. Any disturbances in the scattering process change the momentum distribution of the spins and are encoded as a phase shift in the precessing polarization. This phase shift results in a loss of the polarization signal. Its application in observing quantum-mechanical behavior of matter waves [7] and slow dynamics of macromolecules [8] shows the very usefulness of this instrument and its potential.

The High-flux Advanced Neutron Application Reactor (HANARO) at Korea Atomic Energy Research Institute (KAERI) has been developing various neutron spectrometers. Primary instruments include Small-Angle Neutron Scattering instrument (SANS), High Resolution Powder Diffractometer (HRPD), Four-Circle Diffractometer (FCD) and Residual Stress Instrument (RSI). However, polarized neutrons were not used until the development of the spin-echo instrument. The spin-echo instrument we are developing is expected to initiate various research

*E-mail: sungmin@kaist.ac.kr

subjects involving polarized neutrons. In this paper, the principles of neutron spin echo [6,9] are briefly reviewed, and the result of a performance test is presented.

II. THEORETICAL BACKGROUND

A polarized neutron spin prepared in the $|+z\rangle$ state is transported along the y direction (Fig. 1). While the neutron is moving in a static magnetic field, $\boldsymbol{B}_1(=B_1\hat{z})$, a $\pi/2$ spin flipper at position **A** (Fig. 1) rotates the spin into a $|+x\rangle$ state which is a superposition of the $|+z\rangle$ and the $|-z\rangle$ states. The spin now begins precessing in the x-y plane around the static field $\boldsymbol{B}_1$. Quantum mechanically, the precession of a spin is a result of two evolving phases of eigen spin states at different rates.

The spin state in a static field can be described by a Schrödinger equation of the following form:

$$\left[-\frac{\hbar^2}{2m}\nabla^2 - \mu\cdot\boldsymbol{B}(\vec{r},t)\right]\Psi(\vec{r},t) = i\hbar\frac{\partial\Psi(\vec{r},t)}{\partial t}, \qquad (1)$$

where $\hbar$ is the Plank constant, and m and μ are the mass and the magnetic moment of the neutron, respectively. The general solution of Eq. 1 can be given as a superposition of two eigenstates of spin 1/2 particles, $|+z\rangle$ and $|-z\rangle$, and the propagation coefficients $f_\pm$:

$$\Psi = \begin{pmatrix}\Psi_+\\ \\ \Psi_-\end{pmatrix} = f_+(\vec{r},t)|+z\rangle + f_-(\vec{r},t)|-z\rangle. \qquad (2)$$

While the total energy of a neutron is conserved, the potential energy for each eigenstate is different in the static magnetic field; thus, the kinetic energy is split into two parts. This is called the Zeeman effect. Therefore, the kinetic energy (or the momentum $\hbar k_\pm$) of the eigenstates in the field is given by the energy conservation equation

$$\frac{\hbar^2k_0^2}{2m} = \frac{\hbar^2k_\pm^2}{2m} - \boldsymbol{\mu}\cdot\boldsymbol{B}, \qquad (3)$$

where $\hbar k_0$ represents the initial momentum with no magnetic field, and $\hbar k_+$ and $\hbar k_-$ are the momenta of the spin-up and the spin-down state, respectively. When the momentum difference caused by the Zeeman split is small compared to the initial momentum, k_0, $k_\pm$ can be calculated to be

$$k_\pm \cong k_0 \mp \frac{m|\mu|B}{\hbar^2k_0}. \qquad (4)$$

The absolute value of magnetic moment μ is indicated because the magnetic moment of a neutron has a negative value. Equation 4 shows that the kinetic energy of a spin-down state is higher than that of a spin-up state. In other words, the spin down state travels faster in the given magnetic field. For neutrons traveling in the y-direction, the wavefunction is then given by

$$\Psi = e^{i[(k_0-\triangle k)y-\omega_k t]}|+z\rangle + e^{i[(k_0+\triangle k)y-\omega_k t]}|-z\rangle, \qquad (5)$$

where $\triangle k \equiv m|\mu|B/\hbar^2k_0$. Therefore, for the neutrons initially polarized along the x-direction, the degree of polarization in the x-direction after the neutron has traversed through a static magnetic field B of path length L is given by

$$\begin{aligned} P_x(B,L) &= \langle\Psi|\sigma_x|\Psi\rangle \qquad (6)\\ &= \int g(k)dk\cos(2L\triangle k)\\ &= \int \tilde{g}(\lambda)d\lambda\cos(\gamma BLm\lambda/h), \end{aligned}$$

where $g(k)$ and $\tilde{g}(\lambda)$ are the momentum and the wavelength distribution functions, respectively. In the momentum distribution function, the momentum split due to the Zeeman effect is neglected ($g(k\mp\triangle k)\cong g(k)$) because, in most cases, the Zeeman shift of the wavevector is much smaller than the neutron momentum distribution width [10]. The oscillating feature of the polarization vector $\boldsymbol{P}$ about the magnetic field is what we call Larmor precession. The quantity γB determines the rotating frequency of the polarization vector and is denoted by ω_L, the Larmor frequency. The gyromagnetic ratio, $\gamma = 2\mu/\hbar$, for a neutron is about 2.916 kHz/Gauss. In Eq. 6, the quantity $2L\triangle k$ describes the accumulated phase difference between spin-up and spin-down states after the neutron has traveled a distance L in a static magnetic field B:

$$\triangle\varphi = 2L\triangle k = \gamma BLm\lambda/h. \qquad (7)$$

Thus the accumulated phase difference between **A** and **B** can denoted as $\triangle\varphi_{AB} = \gamma B_1L_1m\lambda/h$ (Fig. 1).

As BL in Eq. 6 increases, the polarization is decreased by the dispersive action; *i.e*, the polarization vectors for different wavelengths precess for different amounts, which results in a vanishing polarization of the beam. The vanished polarization can be recovered by using a π spin flipper at **B** to reverse $\triangle\varphi_{AB}$ (Fig. 1), and by subsequently letting the spin phases evolve again in a static field B_2 of path length L_2. Thus, at point **C**, the total accumulated phase difference between two spin states is

$$\triangle\varphi_{total} = \triangle\varphi_{BC} - \triangle\varphi_{AB} = \gamma(B_2L_2 - B_1L_1)m\lambda/h. \qquad (8)$$

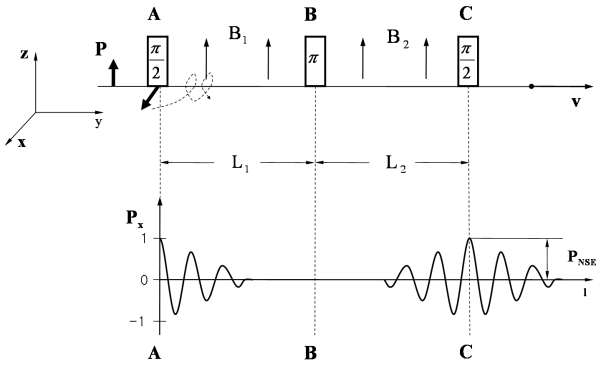

Fig. 1. Diagram of the standard spin-echo principle [6].

If the configuration is symmetric ($B_1L_1 = B_2L_2$), the phase difference, $\triangle\varphi_{total}$, will be zero for all wavelengths, and the polarization P_x will be fully recovered. The polarization, P_x, is then measured by projecting the spin-up component on to an analyzer after the polarization has been rotated back in z direction by using a $\pi/2$ flipper at **C** (Fig. 1).

The amplitude of the P_x oscillation at the symmetry position **C** is called the "spin echo signal," P_{NSE}. The spin-up and the spin-down states take different times to travel through the field because the velocities of the two states (initially given by v_0) in a static magnetic field are given by

$$v_{\pm} = v_0 \pm \frac{\hbar\omega_L}{2mv_0}. \tag{9}$$

Then, the relative time difference for the two states to travel through the field can be obtained as

$$\begin{aligned}\triangle t = t_+ - t_- &= \frac{L}{v_+} - \frac{L}{v_-} = \frac{\hbar\omega_L L}{mv_0^3} \\ &= \frac{2|\mu|BL}{mv_0^3} = \tau_{NSE}.\end{aligned} \tag{10}$$

Therefore, another useful constant, τ_{NSE}, is defined and called the "spin-echo time" [9]. In inelastic measurements, this constant determines the accessible time range.

III. EXPERIMENT AND RESULTS

The schematic and the picture of the spin-echo instrument at the ST-1 beam port of HANARO are shown in Fig. 2 and Fig. 3, respectively. The thermal neutron flux of ST-1 port was 1.8×10^{14} n/cm^{2}sec prior to the monochromator. After the polarizer (monochromator) and the 1-cm-diameter collimator, the neutron flux was reduced to 5.7×10^4 n/cm^{2}sec. A $Co_{0.92}Fe_{0.08}$ ferromagnetic single crystal (50 mm(W) × 50 mm(H) × 3 mm(T)) was used as a monochromatic polarizer and an analyzer [11]. At the Bragg condition of the (200) lattice plane, the crystal reflects $|+z\rangle$ states and transmits $|-z\rangle$ states. When the 20° ($2\theta = 40°$) of Bragg angle of the polarizing crystal was used, monochromatic (1.2 Å) neutrons

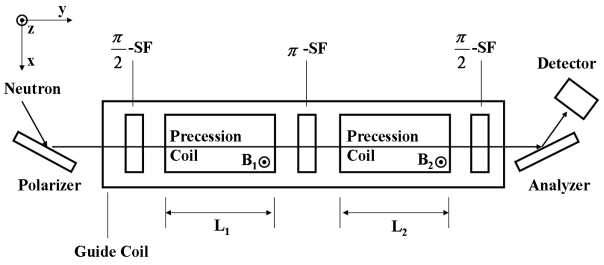

Fig. 2. Arrangement of a Mezei type neutron spin echo instrument. In the experiment, the symmetry condition ($L_1 = L_2 = 30$ cm) was satisfied.

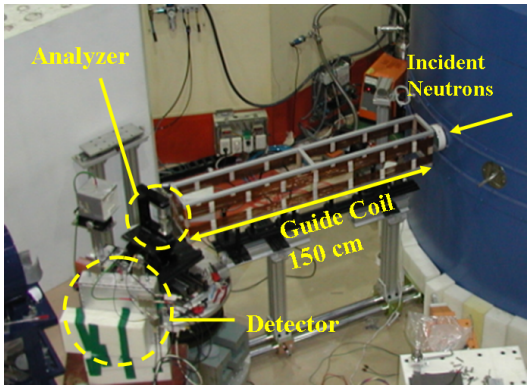

Fig. 3. The spin echo instrument located at ST-1 beam port of HANARO. Spin flippers and precession coils are located inside the guide coil. Permanent magnets are used inside the beam port to maintain the neutron spin polarization.

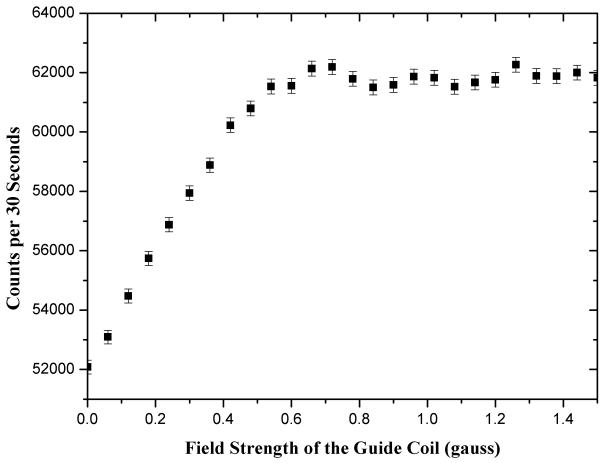

Fig. 4. Neutron intensity as a function of the guide field strength.

polarized in $|+z\rangle$ states were obtained. Two consecutive sessions of static magnetic fields along the $+z$ direction, which are called guide fields, were used to maintain the spin polarization along the entire beam path. A magnetic field produced by a series of permanent magnets was used for the first guide field. The second guide field was generated by using a guide coil. The number of neutrons with $|+z\rangle$ states was measured as a function of guide field strength (Fig. 4) by using a ^{3}He position sensitive detector. As the magnetic field strength of the guide coil was increased, the number of neutrons arriving at the analyzer with $|+z\rangle$ states initially increased and then became saturated above a 0.6-Gauss guide field. In other words, the polarization of neutrons was not maintained when the guide field was off, and a few Gauss was enough to keep spins from depolarizing due to unwanted magnetic fields, such as the earth's magnetic field.

Two kinds of Mezei-type [6,12] spin flippers were used in this experiment. A Mezei-type flipper (Fig. 5) consists of two orthogonally oriented coils producing two perpen-

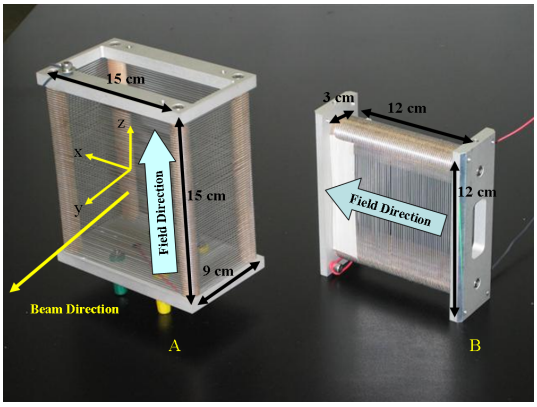

Fig. 5. Picture of a neutron spin flipper. The coils produce magnetic fields perpendicular to each other. When coil B is assembled inside coil A, coil A cancels the guide field within the flipper, and Coil B provides the x-direction magnetic field B_x.

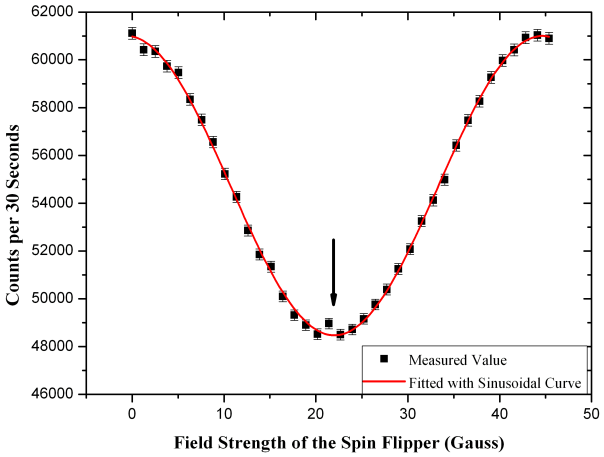

Fig. 6. Neutron intensity as a function of the spin flipper field strength. The π spin flipping occurred when B_x was 22.0 Gauss (arrow).

dicular magnetic fields, one in the $-z$ direction and the other in the $+x$ direction. The magnetic field in the $-z$ direction cancels the guide field within the flippers. As a result, only the $+x$ direction field is left inside the flipper to rotate spins around the x axis. Thus, if the field strength, B_x, and the time, t, that the spin resides within the field satisfies a flipping condition, we have a π spin flipper ($\gamma B_x t = \pi$) or $\pi/2$ spin flipper ($\gamma B_x t = \pi/2$). For a given path length within the flipper, the angle of rotation can be varied by the strength of B_x.

To find field strengths B_x that satisfies the π and the $\pi/2$ flipping conditions, we counted the number of neutrons arriving at the detector as a function of the current supplied to the flipper coil that produced B_x. The spin flip coil was located in the beam path where a weak guide field ($\sim$ 1 Gauss) was generated by the guide coil. Thus, neutron spins initially polarized along the z direction were rotated about B_x of the spin flipper, and the angle of rotation was determined by using the amplitude of $|+z\rangle$ spin state. This amplitude was measured by projecting the spin state onto the analyzer and then counting the neutrons arriving at the detector. The field strength for π flipping can be identified as the minimum point in Fig. 6 and was found to be $B_{x,\pi} = 22.0$ Gauss (3.49-A spin-flipper coil current). Thus, the $\pi/2$ flipping field strength is $B_{x,\frac{\pi}{2}} = B_{x,\pi}/2 = 11.0$ Gauss (1.75-A spin-flipper coil current). From this experiment, the flipping ratio was measured to be 1.26, where the flipping ratio was defined as the ratio of neutron intensities in the ON and the OFF status of the π spin flipper (I_{OFF}/I_{ON}). In addition, the spin flipper efficiency and the polarizer-analyzer efficiency product were measured using a two π spin flipper method [13]. This method describes the polarizer-analyzer efficiency product P_1P_2 and the spin-flipper's efficiencies f_1, f_2 as

$$P_1P_2 = R_{12}(R_1-1)(R_2-1)/(R_1R_2-R_{12}), \qquad (11)$$
$$f_i = (R_i-1)(1+P_1P_2)/2P_1P_2R_i\ ,$$

where R_1 and R_2 are the flipping ratios of the two different spin flipper (SF_1 and SF_2), and R_{12} is the flipping ratio when two π spin flippers are used simultaneously. The polarizing (analyzing) efficiency, P_1 (P_2) is defined as $P = (\tau^+ - \tau^-)/(\tau^+ + \tau^-)$ where τ^+ and τ^- are transmissions for neutrons with $|+z\rangle$ and $|-z\rangle$ states, respectively. From the measurements with four different combinations of two spin flippers, all the R values were obtained as follows:

$$R_1 = I_{SF1\ OFF,\ SF2\ OFF}/I_{SF1\ ON,\ SF2\ OFF}, \qquad (12)$$
$$R_2 = I_{SF1\ OFF,\ SF2\ OFF}/I_{SF1\ OFF,\ SF2\ ON},$$
$$R_{12} = I_{SF1\ OFF,\ SF2\ OFF}/I_{SF1\ ON,\ SF2\ ON}.$$

From these values and Eq. 11, the efficiency of the spin flippers (f_i) and the polarizer-analyzer efficiency product (P_1P_2) were estimated to be 0.98 ± 0.01 and 0.14 ± 0.01, respectively. In this case, the neutron polarization after the polarizer (P_1) was calculated to be approximately 0.37 if identical efficiencies ($P_1 = P_2$) are assumed for the polarizer and the analyzer.

After the field strengths of the spin flippers had been determined, the spin phase evolution was measured using three spin flippers and two precession coils within a guide coil (Fig. 2). Each precession coil producing a static field in the $+z$ direction was located between $\pi/2$ and π flippers. Incident neutron spins polarized along the $+z$ direction were rotated into the transverse plane by the first $\pi/2$ spin flipper. In the first subsequent precession coil, neutron spins precessed about the $+z$ direction during the 30-cm flight within the coil. The amount of phase evolution was determined by B_1 and L_1 of the precession coil (Eq. 7). Then, the phase evolution in the first precession coil was reversed by the π spin flipper and compensated for by the second precession coil (B_2, L_2), resulting in polarization recovery. The recovered polarization P_x was rotated by the last $\pi/2$ spin flipper, and the amplitude of $|+z\rangle$ was measured by using the ana-

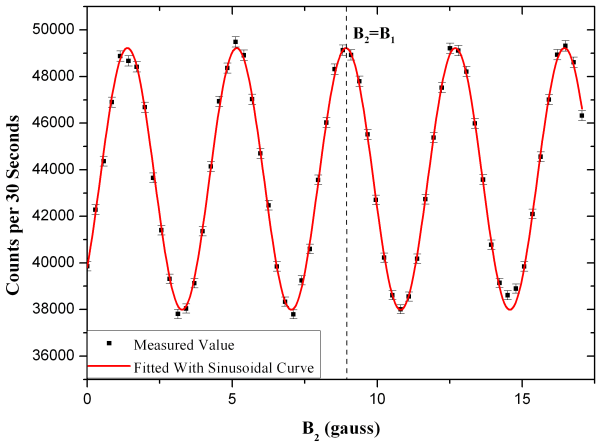

Fig. 7. Spin-echo signal as a function of the second precession coil field strength B_2. During the measurement, B_1 was kept constant at 8.96 Gauss. The spin-echo condition is indicated by a dotted line. A sinusoidal fitting showed that the amount of spin phase evolution up to the echo point was 14.8 rad.

lyzer and detector. To find the spin echo point, we varied B_2 while keeping B_1 constant at 8.96 Gauss. The result is shown in Fig. 7. Since highly monochromatic neutrons were used, the wavelength distribution function in Eq. 6 could be replaced by the delta function $g(\lambda) \cong \delta(\lambda - 1.2$ Å). The oscillating feature of the polarization vector, the phase evolution of a neutron spin, is then explained by using a sinusoidal function. An analysis with the sinusoidal function resulted in a 14.8-rad spin phase evolution up to the echo point (Fig. 7), which corresponded to the expected phase evolution (14.9 rad) given by Eq. 7 with $B_1 = 8.96$ Gauss and $L_1 = 30$ cm. Therefore, the spin echo condition $B_1 L_1 = B_2 L_2$ was satisfied.

According to Eq. 10, τ_{NSE} of our spin-echo instrument, which determines the accessible time range in inelastic measurement, is in the range of a few picoseconds. Since the spin-echo time is proportional to $B\lambda^3$, a longer spin-echo time (a few tens of nanoseconds) may be achieved using longer wavelength neutrons and higher precession fields.

IV. CONCLUSION

A neutron spin-echo instrument with a spin-echo time of a few picoseconds was developed at HANARO for the first time in Korea, and the phase evolution of a neutron spin state was observed (Fig. 7). The measured spin-echo point was in agreement with the expected value. The efficiency of the developed spin flipper ($f \cong 0.98$) and the polarizer-analyzer efficiency product ($P_1 P_2 \cong 0.14$) were measured. The low measured polarizer-analyzer efficiency product indicates that the low contrast of the spin-echo signal was due to the poor polarizing power of the crystal. With further development, the spin-echo instrument should be capable of being used as a spin interferometer [14,15] or an inelastic neutron spectrometer [16]. A different type of spin-echo instrument is also being developed using RF flippers [17,18]. Further development of the spin echo instrument at HANARO may bring new research opportunities to the neutron science community in Korea.

REFERENCES

[1] R. Kiyanagi, H. Kimura, M. Watanabe, Y. Noda, T. Mochida and T. Sugawara, J. Korean Phys. Soc. **46**, 239 (2005), Chap. 1.
[2] R. J. Birgenau, D. E. Moncton and A. Zeilinger, *Frontiers of Neutron Scattering*, (North-Holland, Amsterdam, 1985).
[3] E. L. Hahn, Phys. Rev. **77**, 297 (1950).
[4] E. L. Hahn, Phys. Rev. **80**, 580 (1950).
[5] F. Mezei, Neutron Spin Echo and Polarized Neutrons, *in Neutron Inelastic Scattering 1977*, (IAEA, Vienna, 1978), p. 125.
[6] F. Mezei, *Neutron Spin Echo, Lecture Notes in Physics*, (Springer-Verlag, New York, 1980), Vol. 128.
[7] S. V. Grigoriev, W. H. Kraan, F. M. Mulder and M. Th. Rekveldt, Phys. Rev. A **62**, 063601 (2000).
[8] P. Schleger, B. Farago, C. Lartigue, A. Kollmar and D. Richter, Phys. Rev. Lett. **81**, 124 (1998).
[9] R. Gähler, R. Golub, K. Habicht, T. Keller and J. Felber, Physica B **229**, 1 (1996).
[10] H. Rauch and S. S. Werner, *Neutron interferometry, Lessons in Experimental Quantum Mechanics*, (Oxford, New York, 2000), Chap. 1.
[11] V. F. Sears, *Neutron Optics*, (Oxford, New York, 1989).
[12] F. Mezei, Z. Physik **255**, 146 (1972).
[13] J. B. Hayter, Z. Physik B **31**, 117 (1978).
[14] S. V. Grigoriev, Yu. O. Chetverikov, A. V. Syromyatnikov, W. H. Kraan and M. Th. Rekveldt, Phys. Rev. A **68**, 033603 (2003).
[15] D. Yamazaki, Nucl. Inst. Meth. Phys. Res. A **488**, 623 (2002).
[16] R. Gähler, R. Golub and T. Keller, Physica B **180-181**, 899 (1992).
[17] R. Gähler and R. Golub, Z. Phys. B **65**, 269 (1987).
[18] R. Golub and R. Gähler, Phys. Lett. A **123**, 43 (1987).